First Results of a Positron Microscope

James Van House and Arthur Rich
University of Michigan, Department of Physics, Ann Arbor, Michigan 48109
(Received 14 July 1987)

We have constructed a prototype transmission positron microscope (TPM) and taken magnified pictures of various objects with it. Information gained from the prototype TPM has allowed us to predict resolutions achievable in the near future with an upgraded TPM. Applications are discussed.

PACS numbers 07.80.+x, 41.80.−y, 61.80.Fe

The transmission electron microscope (TEM) when originally introduced had as a major goal the exploitation of the high resolution made possible by subangstrom de Broglie wavelengths. During the past decades angstrom resolutions have finally been realized, but perhaps of equal interest, a number of new types of electron microscopes, such as the scanning transmission, scanning tunneling, and field-emission microscopes, have been used in a variety of imaging applications, some at resolutions as low as 1 μm. In addition, a number of microscopes using other particles (various types of ions[1] and the neutron[2]) have been developed. These latter devices have as their goal image formation resulting in a different contrast, as well as possibly higher resolution than that obtained with the use of electrons.

In this Letter we present the first results obtained with the positron (e^+) as the imaging particle in a transmission microscope. The transmission positron microscope (TPM) should have a variety of new applications as a result of the different contrast which appears when e^+ rather than e^- are used as the imaging particle. Our instrument uses a slow e^+ beam which, when combined with "positron" optics appropriate to the slow e^+ emittance, and the use of image analysis techniques, has permitted us to construct the first TPM, compare its properties to our calculations, and obtain magnified images of several thin films. The purpose of our Letter is to detail the above features and to discuss the new applications referred to above.

The success of our instrument is partially based on the fact that the brightness of an e^+-emitting radioactive source, initially too low for imaging, is increased enormously by a process called moderation.[3] In this process the initially high-energy ($\simeq$100–500 keV) source e^+ thermalize in, for example, a W crystal and, with probability 10^{-3}–10^{-4}, are ejected at an energy of about 2 eV. The ejected e^+ are then formed into a beam. The e^+ moderation process and the formation of slow e^+ beams is now a standard technique.[3]

Our e^+ beam optics (Fig. 1) focuses 3.5×10^5 e^+/sec into a 1.7-mm spot at the target. The e^+ transmitted through the target are imaged by an objective lens and then by a projector lens onto a three-plate channel electron-multiplier array (CEMA) with a phosphor-screen anode. The CEMA-phosphor combination converts each e^+ into a spot of light which is detected by an image-analysis system (Fig. 1). The system adds the event to the appropriate memory location in a 384×384 array, resulting in a digital signal averaging which is crucial to our initial results, since it allows an image to be built up at rates as low as 200 Hz.

Resolution of the transmission positron microscope.—In the paraxial approximation, the spatial resolution in object space of the objective lens (where aberrations affect the image most strongly), under the condition that the magnification $M \gg 1$, can be expressed[4] as

$$R = \tfrac{1}{4} C_s \alpha^3 + C_c \Delta E \alpha / 3E. \quad (1)$$

Here C_s and C_s are the spherical and chromatic aberration coefficients of the lens, E is the energy of the beam at the target, and ΔE is the variation in E ($\Delta E \ll E$). The half-angle α is the acceptance angle of the lens, determined in our system by the contrast aperture shown in Fig. 1. The beam incident on the lens has an angular spread α' which is determined by the initial phase space of the beam at the moderator, as well as by the optics used to accelerate, transport, and focus the beam onto

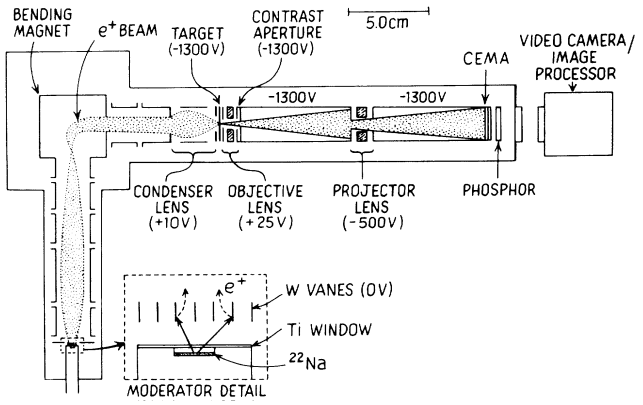

FIG. 1. The transmission positron microscope. Positrons (e^+) from a ^{22}Na source are incident on a W vane moderator. The reemitted slow e^+ are focused into a beam which is transported to a bending magnet. The beam is subsequently incident on a low-aberration condenser lens which focuses it onto the target.

the target. If $\alpha' \leq \alpha$, R will be determined by α', which should then be used in Eq.(1) rather than α.

In the TEM, R is determined by a minimization of the combination of lens aberrations [Eq.(1)] and diffraction spreading [$R_d = 0.6\lambda/\alpha$ with $\lambda = h(2mE)^{-1/2}$ the de Broglie wavelength], giving a limit on R (with neglect of chromatic aberrations) of $R^{dl} = 0.4 C_s^{1/4} \lambda^{3/4}$ which, at $E = 100$ KeV and $C_s \simeq 2$ mm, is about 2 Å.[5] In the TPM, because of low beam brightness, R is currently limited by statistics rather than by R^{dl} so that beam and detector properties must be considered. The optimization of R for the TPM involves our restricting α (or α') until the detector counting rate is the minimum required to form an image in a reasonable time. With these considerations, and in view of the rapid development of both slow e^+ beam-generation and imaging technology, we will present Eq.(1) in a form which allows us to determine R for a wide variety of possible beam and detector configurations.

We first relate the acceptance angle α (assumed small) to the beam current density ρ_d at the detector ($\rho_d = I_d/A_d$, where A_d and I_d are the beam area and the current at the detector, respectively) and to the current density ρ_m at the moderator ($\rho_m = I_m/A_m$ where A_m is the moderator area and I_m the moderated-positron current). If θ_m is the spread in emission angle of positrons from the moderator, E_m the emission energy, E the beam energy at the target, and M the system magnification, then, using Liouville's theorem,[6] we find

$$\alpha = \left(\frac{\rho_d}{\rho_m} \frac{E_m}{E} \right)^{1/2} M \sin\theta_m . \tag{2}$$

The value of M is determined by the detector resolution. This is because, if $R = 0$, the minimum resolvable feature on the detected image would be given by $r_d = MR_d$, where r_d is the diameter of a single-particle image produced by the CEMA and R_d the corresponding detector resolution referred back to the object. Since R and R_d are independent, the overall system resolution, R_m, is the quadrature sum of R and R_d. An approximate optimization of R_m under our conditions of low beam rate occurs when $R = R_d$. If we use $M = r_d/R$ and substitute Eq.(2) into Eq.(1), solution of the resulting quartic in R yields

$$R = \left[\frac{C_c}{6} \left(\frac{\Delta E}{E} \right) \left(\frac{E_m}{E} \right)^{1/2} \sin\theta_m \left(\frac{\rho_d}{\rho_m} \right)^{1/2} r_d \left\{ 1 + \left[1 + \frac{9 C_s r_d \sin\theta_m [(\rho_d/\rho_m)(E_m/E)]^{1/2}}{(C_c \Delta E/E)^2} \right]^{1/2} \right\} \right]^{1/2} . \tag{3}$$

In the case where spherical aberrations dominate R, which commonly occurs in the TEM,[5] Eq.(3) simplifies to

$$R = \left(\frac{C_s}{4} \right)^{1/4} \left(\frac{\rho_d}{\rho_m} \frac{E_m}{E} \right)^{3/8} (r_d \sin\theta_m)^{3/4} . \tag{4}$$

The verification of the above analysis is crucial to further development of the TPM. Our experiment has confirmed the analysis (see next section); however, before a detailed presentation of our specific results, we give a more general discussion applicable to a wider range of current and proposed technologies.

The parameter ρ_d is set by the dual criteria that it yield an image with sufficient statistics to give good contrast in a reasonable time as well as being acceptably above the detector dark noise. These criteria, in turn, are partially determined by r_d, as well as the image format. We calculate, for a 256×256 image format, $r_d = 4 \times 10^{-3}$ cm (which can be achieved with a CEMA), and a 10-h running time, that $\rho_d = 1.6 \times 10^{-17}$ A/cm^2 is required for good image contrast. The values E_m and $\sin\theta_m$ vary widely.[3] For our calculation we use the properties of the W single-crystal moderator which has $E_m = 2.2$ eV, $\theta_m = 20°$, and $\Delta E = 0.08$ eV,[7] and we take $C_s = 2$ mm, which is typical of magnetic lenses used in the TEM.[5] Because of the small ΔE, chromatic aberrations are small and we can apply Eq.(4), using the above numerical values to calculate $R(\rho_m)$ for $E = 1$, 10, and 100 keV (Fig. 2). Also shown in Fig. 2 is the current density, ρ_m^{dl}, at which $R(\rho_m) = R^{dl}$. Since R^{dl} and R both scale as $E^{-3/8}$, ρ_m^{dl} is independent of energy. For $\rho_m > \rho_m^{dl}$, no further improvement in R is obtained; however, running time for a given R decreases as ρ_m increases.

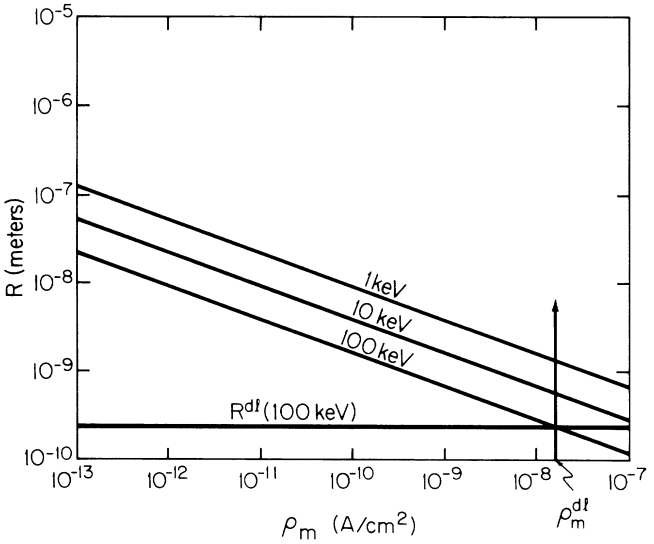

FIG. 2. The expected resolution of the TPM under conditions discussed in the text. Also shown is the diffraction-limit current density, ρ_m^{dl}, and the resolution limit due to diffraction, R^{dl}, at 100 keV.

In this example, R^{dl} occurs at $\rho_m^{dl}=1.6\times10^{-8}$ A/cm^2. At the present time the reactor-based Brookhaven National Laboratory's beam[8] has the highest value of ρ_m so far achieved (6×10^{-12} A/cm^2) which we predict would give $R=5$ nm at 100 keV. Higher ρ_m should be obtained in the future at Brookhaven National Laboratory[8] or with the larger reactors of the Idaho National Engineering Laboratory,[9] while beams suitable for use in a standard laboratory setting with $\rho_m\sim5\times10^{-12}$ A/cm^2 are now envisioned.

Experimental Results.—As previously stated, we feel that it is crucial to verify Eqs.(3) and (4) so that future and more powerful TPM's, as well as other types of e^+ microscopes, can be constructed. We thus analyze in some detail the prediction of R for our instrument and its comparison with experiment.

The values of our TPM parameters are $C_s=4.3$ cm, $C_c=2.4$ cm,[4] $\rho_m=(2.4\pm1.2)\times10^{-13}$ A/cm^2, $\sin\theta_m=1$, $E_m=2$ eV, and $\Delta E\simeq2$ eV, and we measured $r_d=(2.0\pm0.5)\times10^{-2}$ cm by taking images of single-particle events. The beam energy, E, was set at 1.3 keV, in order to demonstrate that the TPM could operate at the low voltages where the largest differences between e^- and e^+ images may appear, as discussed below. We set $\rho_d=1.6\times10^{-17}$ A/cm^2, 16 times the CEMA dark noise. Using the above values in Eq.(3), we predict $R=1.6\pm0.5$ μm, and to match this resolution to r_d we set $M=r_d/R=125$. A contrast aperture (Fig. 1) restricts α to the 3° required to achieve $r=1.6$ μm. The predicted (total) measured resolution R_m, the quadrature sum of the lens resolution and the (equal) detector resolution R_d, is $R_m=2.2$ μm.

Images were obtained for polyvinyl-acetate-chloride copolymer (VYNS)[10] foils less than 800 Å thick (upper limit determined from optical interferometry techniques) supported on a 100-line, 82% transmitting copper mesh. The use of the films allowed us to determine the unknown effects of inelastic scattering on the chromatic aberration term in Eq.(3). At these thicknesses, (20–50)% of the incident beam was transmitted, leading us to estimate, from e^+ range measurements,[3] that the actual target thicknesses were 200–400 Å. Images of various targets were taken at $M=55\times$, $75\times$, and $100\times$. The best contrast is obtained at $M=55\times$. One such image is shown in Fig. 3. It required 4 h of signal averaging to accumulate. The magnification was calibrated from the known 250-μm grid wire spacing. Gaussian fits to a histogram of one of the grid wires in Fig. 3 with and without VYNS film yielded respectively (errors are statistical) $R_m=9\pm1$ and 4.5 ± 0.5 μm. The latter is in agreement with the predicted value $R_m=4\pm1$ μm. We conclude that the predictions of Eq.(3) are verified to within experimental error and that chromatic aberrations due to inelastic scattering in the target degrade the resolution by only a factor of 2. Such an effect is not serious enough to prevent the use of the TPM at energies down to 1 keV.

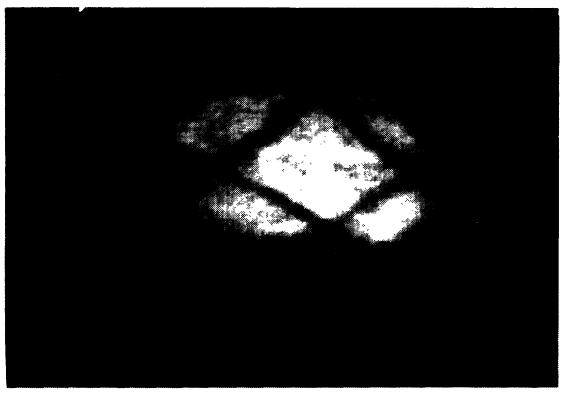

FIG. 3. The first TPM picture. The photograph is a VYNS film, taken at 55 times magnification. The image was obtained after adjustment of the objective lens voltage until the filamentary structure of the unbroken areas of the foil between the grid wires (spacing 250 μm) was in focus. The brightest areas are tears in the fragile VYNS film.

Applications of the TPM.—Because of the opposite sign of the Coulomb interaction, a number of well-known differences exist between e^+ and e^- in their scattering interactions with matter in the energy range (1 keV $<E<1$ MeV) and angular range ($\theta<5\times10^{-2}$ rad) of interest. Comparison of the resulting contrast differences between TEM and TPM images taken under otherwise identical conditions could help isolate the effects of particular terms in the scattering cross section on image formation in a manner which cannot be done with the TEM alone. In particular, for $E<100$ keV, the screening of the nucleus is more effective for $e+$, resulting in a substantially reduced small-angle scattering.[11] Using the method of Lentz[12] and the e^+ vs e^- Thomas-Fermi screening angles,[11] we calculate that, at $E=50$ keV, a strongly Z-dependent (Z is the atomic number) fractional difference in the amplitude contrast, ranging from 10% for $Z=8$ to 130% for $Z=80$, exists between the TPM and TEM. These differences should be 2–3 times larger at lower energies.[13] Comparison of the contrast differences (once they are calibrated) between TPM and TEM images may provide information on atomic form factors due to the screening differences,[13] and could eventually, because of the strong Z dependence, prove a sensitive microanalysis technique. The strong repulsion of the e^+ by the nuclear charge will also alter the phase shifts of the partial waves compared to e^-.[14] This will result in differences in the phase contrast which could be as large as those calculated above for the amplitude contrast. A further consequence of the suppressed elastic scattering is a factor of 1.3 increase in the ratio of the e^+ to e^- range for $E>100$ keV.[15] As a result, thicker targets or lower energies can be used in the TPM for a given contrast.

In addition to the above effects in the elastic scattering, the inelastic cross section is predicted[16] to increase for e^+ compared to e^- by as much as 15% at $E < 100$ keV, as a result of a term proportional to Z^3, altering the relative contributions of elastic and inelastic scattering to the contrast in the TPM. The increased inelastic scattering also results in a larger energy loss per unit length for e^+ vs e^-. As a consequence, the secondary e^- intensity produced from thin targets will be increased and the spectral composition altered when e^+ rather than e^- are incident on the target. When combined with a secondary e^- analysis technique the TPM should provide a different sensitivity to target composition from that of the TEM. Finally, major differences are predicted to occur between e^- and e^+ diffraction contrast at energies up to 1 MeV.[17] Comparison of these differences might help to resolve questions concerning defect formation in materials.[18]

We are also analyzing a number of smaller effects which occur for $E > 50$ keV which could also prove to be of utility.[15] Among these are several new signals which have no analog in the TEM, but which will appear in the TPM as a result of e^+ annihilation in flight. These signals contain information on the binding energies and momentum-space distribution of the target electrons.[15] They are annihilation of the e^+ in the target into two γ rays,[19] annihilation into a single γ ray with the emission of a coincident x-ray,[19] radiationless annihilation with the emission of a high-energy electron,[20] and positron-electron capture.[21]

In conclusion, we have taken the first transmission positron microscope pictures and verified our predictions of the resolution. As discussed above, several substantial differences should exist between the TEM and TPM. Our experience with the prototype TPM should be applicable to the proposed e^+ reemission microscope[17] and possibly to the recently demonstrated e^+ microprobe,[22] and has allowed us to design and begin construction of an instrument with sufficient current density to allow TPM resolutions approaching the diffraction limit.

We acknowledge useful discussions with L. Allard, W. Bigelow, G. Brooks, R. Conti, W. Parkinson, G. Rempfer, M. Skalsey, and P. Zitzewitz, and we thank N. Hadari and M. Massey for contributions in the initial phases of the research. We particularly thank W. Frieze and D. W. Gidley for a critical analysis of the manuscript and for helpful discussions of the research.

Research on the positron microscope was supported by the National Science Foundation (Grant No. PHY 9403817) and the University of Michigan under a grant from the Office of the Vice President for Research.

[1]R. Levi-Setti, Adv. Electron. Electron Phys. Suppl. **13C**, 261 (1980); R. Levi-Setti *et al.*, Phys. Rev. Lett. **54**, 2615 (1985).

[2]P. Herrmann *et al.*, Phys. Rev. Lett. **54**, 1969 (1985).

[3]For a general review see A. P. Mills, Jr., in *Positron Solid State Physics,* International School of Physics "Enrico Fermi," Course LXXXIII, edited by W. Brandt and A. Dupasquier (North Holland, Amsterdam, 1983).

[4]G. F. Rempfer, J. Appl. Phys. **57**, 2385 (1985).

[5]B. Siegel, in *Modern Developments in Electron Microscopy,* edited by B. Siegel (Academic, New York, 1964), Chap. 1.

[6]*Applied Charged Particle Optics,* edited by A. Septier (Academic, New York, 1980).

[7]D. A. Fischer, Ph.D. thesis, State University of New York at Stony Brook, 1984 (unpublished).

[8]K. G. Lynn and A. P. Mills, Jr., private communication.

[9]E. Ottewitte and H. Makowitz, private communication; E. H. Ottewitte, in *Advance Accelerator Concepts—1986,* edited by F. E. Mills, AIP Conference Proceedings No. 156, (American Institute of Physics, New York, 1987).

[10]D. W. Green, J. Sci. Instrum. **38**, 333 (1981).

[11]B. P. Nigam and V. S. Mathur, Phys. Rev. **121**, 1577 (1961).

[12]F. Lentz, Z. Naturforsch. **9**, 185 (1954).

[13]I. J. Feng, R. H. Pratt, and H. K. Tseng, Phys. Rev. A **24**, 1358 (1981).

[14]D. P. Dewangen and H. R. J. Walters, J. Phys. B **10**, 637 (1977).

[15]R. D. Evans, *The Atomic Nucleus,* (McGraw-Hill, New York, 1955), Chaps.18–21, and references therein.

[16]J. C. Ashley, R. H. Ritchie, and W. Brandt, Phys. Rev. B **5**, 2393 (1972).

[17]L. D. Hulett, Jr., J. M. Dale, and S. Pendyala, Mater. Sci. Forum **2**, 133 (1984).

[18]D. Van Aken and J. Mansfield, private communication.

[19]W. Heitler, *The Quantum Theory of Radiation* (Oxford Univ. Press, London, 1954), 3rd ed.

[20]N. F. Mott and H. S. W. Massey, *The Theory of Atomic Collisions* (Clarendon, Oxford, 1965).

[21]J. H. McGuire, in *Positron (Electron)-Gas Scattering,* edited by W. E. Kauppila, T. S. Stein, and J. M. Wahdehra, (World Scientific, Singapore, 1986), p. 222.

[22]G. R. Brandes *et al.*, Bull. Am. Phys. Soc. **32**, 439 (1987).

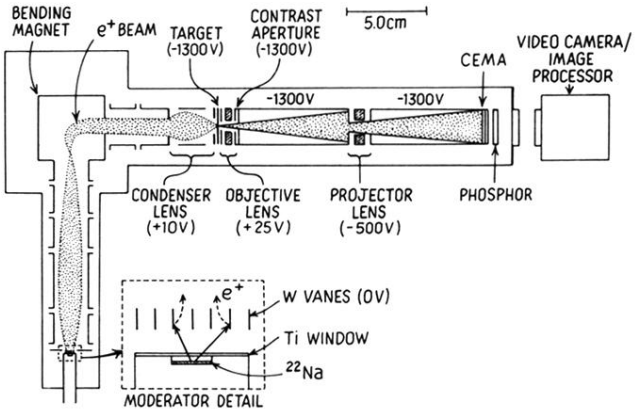

FIG. 1. The transmission positron microscope. Positrons (e^+) from a ^{22}Na source are incident on a W vane moderator. The reemitted slow e^+ are focused into a beam which is transported to a bending magnet. The beam is subsequently incident on a low-aberration condenser lens which focuses it onto the target.

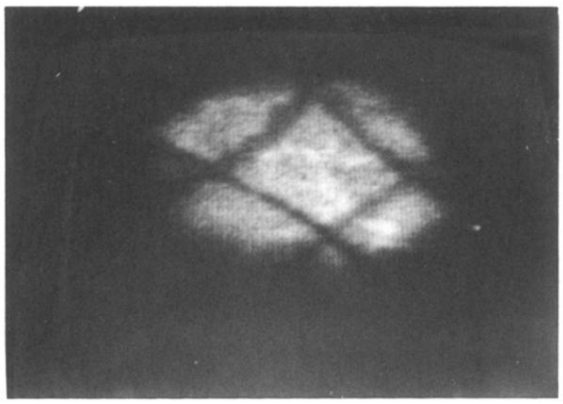

FIG. 3. The first TPM picture. The photograph is a VYNS film, taken at 55 times magnification. The image was obtained after adjustment of the objective lens voltage until the filamentary structure of the unbroken areas of the foil between the grid wires (spacing 250 μm) was in focus. The brightest areas are tears in the fragile VYNS film.